Spectromicroscopy of boron in human glioblastomas following administration of $Na_2B_{12}H_{11}SH$

B. Gilbert,[1,*] L. Perfetti,[1] O. Fauchoux,[1] J. Redondo,[1] P.-A. Baudat,[1] R. Andres,[2] M. Neumann,[3] S. Steen,[3]
D. Gabel,[3] Delio Mercanti,[4] M. Teresa Ciotti,[4] P. Perfetti,[5] G. Margaritondo,[1] and Gelsomina De Stasio[5,6]

[1]*Institut de Physique Appliquée, Ecole Polytechnique Fédérale, PH-Ecublens, CH-1015 Lausanne, Switzerland*
[2]*Paul Scherrer Institut, CH-5232 Villigen, PSI, Switzerland*
[3]*Department of Chemistry, University of Bremen, P.O. Box 330 440, D-28334 Bremen, Germany*
[4]*Istituto di Neurobiologia del CNR, Viale Marx 15, 00100 Roma, Italy*
[5]*Istituto di Struttura della Materia del CNR, Via Fosso del Cavaliere, 00137 Roma, Italy*
[6]*Department of Physics, University of Wisconsin-Madison and Synchrotron Radiation Center,*
3731 Schneider Drive, Stoughton, Wisconsin 53589

Boron neutron capture therapy (BNCT) is an experimental, binary treatment for brain cancer which requires as the first step that tumor tissue is targeted with a boron-10 containing compound. Subsequent exposure to a thermal neutron flux results in destructive, short range nuclear reaction within 10 μm of the boron compound. The success of the therapy requires than the BNCT agents be well localized in tumor, rather than healthy tissue. The MEPHISTO spectromicroscope, which performs microchemical analysis by x-ray absorption near edge structure (XANES) spectroscopy from microscopic areas, has been used to study the distribution of trace quantities of boron in human brain cancer tissues surgically removed from patients first administered with the compound $Na_2B_{12}H_{11}SH$ (BSH). The interpretation of XANES spectra is complicated by interference from physiologically present sulfur and phosphorus, which contribute structure in the same energy range as boron. We addressed this problem with the present extensive set of spectra from S, B, and P in relevant compounds. We demonstrate that a linear combination of sulfate, phosphate and BSH XANES can be used to reproduce the spectra acquired on boron-treated human brain tumor tissues. We analyzed human glioblastoma tissue from two patients administered and one not administered with BSH. As well as weak signals attributed to BSH, x-ray absorption spectra acquired from tissue samples detected boron in a reduced chemical state with respect to boron in BSH. This chemical state was characterized by a sharp absorption peak at 188.3 eV. Complementary studies on BSH reference samples were not able to reproduce this chemical state of boron, indicating that it is not an artifact produced during sample preparation or x-ray exposure. These data demonstrate that the chemical state of BSH may be altered by *in vivo* metabolism.

PACS number(s): 87.59.$-$e

I. INTRODUCTION

Glioblastoma multiforme is the most malignant form of glioma (cancer of the glial cells, which provide the support environment for neurons) and conventional treatments remain incapable of significantly prolonging life expectancy beyond an average of 6–12 months after diagnosis. Radiotherapy after surgery is the only treatment shown to be capable of slowing but not curing the cancer. The significant limitation of radiotherapy or chemotherapy is the lack of specificity towards individual cancer cells, especially when metastasis has occurred. New modalities are sought which target tumor and spare healthy tissue. Glioblastomas appear very heterogeneous, and multiple genetic pathways may lead to the malignant tumor [1] but tumor cells may present different antigens than healthy tissue or amplify certain gene expression. Radioactive isotopes, foreign genes in liposomes or stimulants to the immune system may be conjugated to antiglioma antibodies. Genetic therapies aim to stimulate the expression of foreign toxic genes, or to inhibit the expression of a tumor-specific gene with an antisense gene. In both cases, the exogenous genetic material must penetrate the tumor membrane by, for example, virus mediated delivery.

Boron neutron capture therapy (BNCT), first proposed in 1936 [2], is another experimental therapy that could potentially destroy tumor regions, but spare healthy tissue. The key feature of successful BNCT is the selective accumulation of a ^{10}B-enriched compound in regions of tumor tissue [3]. Neutron capture by ^{10}B leads to fission by the reaction ^{10}B$(n,\alpha)^7$Li. ^{10}B has a capture cross section for thermal neutrons (3,838 b) many times greater than other elements present in tissue (^{16}O has 0.00019, ^{12}C has 0.0035, ^{1}H has 0.333, ^{14}N has 1.83 barn). Therefore, if ^{10}B is present in tissue irradiated by a neutron flux, almost all of the radiation dose results from the boron neutron capture reaction. The energetic alpha and ^{7}Li particles that are produced are highly biologically destructive over a short distance around the boron atom. The ^{7}Li particle has a range of about 3 μm, while the α particle has a range of about 10 μm; both distances are smaller than typical brain cell dimensions. Thus if compounds containing ^{10}B can be delivered only to regions of tumor tissue, irradiation of a macroscopic tissue area with a neutron flux will result in the selective destruction of tumor, while neighboring tissue receives a much lower radiation dose.

Following the administration of a boron compound, it is of great importance to assess its subsequent distribution, in the blood stream, areas of healthy tissue and the tumor itself. Using the technique of inductively coupled plasma atomic

---

*Author to whom correspondence should be addressed.

emission spectroscopy (ICP-AES) to measure volume-averaged boron concentrations, several compounds have demonstrated tumor affinity in animals and humans [4]. One such compound is BSH ($Na_2B_{12}H_{11}SH$), first proposed for BNCT in 1967 [5]. BSH has had some success in the treatment of malignant human gliomas with BNCT in Japan [6] and has been chosen as the compound to be used in European clinical trials [7,8] which were started in 1997. The development of so-called ''third generation'' boron compounds is ongoing, and applies a more systematic methodology common to all antitumor drug design [9] and faces the same challenges, such as the low permeability of the blood-brain barrier.

Because of the short range of the fission products of the boron neutron capture reaction, it is also vital to study the boron distribution in tissue at a microscopic level. A BNCT compound must target all tumor cells to ensure tumor destruction without the possibility of recurrence. Additionally, the location of boron in cells (e.g., cytoplasm or nucleus) has large implications for the efficacy of BNCT treatment. The microdistribution of BSH has been investigated by several techniques [10–12] but no complete description exists of the fate and distribution of BSH *in vivo*. The present study was stimulated by the need to address this important subject for BNCT.

The MEPHISTO (microscope à emission de photoélectrons par illumination synchrotronique de type onduleur) spectromicroscope employs the technique of synchrotron x-ray photoelectron emission spectromicroscopy (X-PEEM), hereafter referred to as spectromicroscopy. MEPHISTO produces magnified images of the area under investigation and performs elemental and chemical state analysis of microareas of the images, while scanning the photon energy. Using tunable soft x rays from a synchrotron source, MEPHISTO acquires x-ray absorption spectra, collecting the electrons emitted at each photon energy from selected areas [13,14]. MEPHISTO micrographs represent the two-dimensional (2D) distribution of the photoelectron emission intensity from the sample surface at a specific photon energy, and provide an image of the area under investigation, on which up to eight spectra can be acquired simultaneously. The field of view of a micrograph can be easily varied between 10 and 500 μm, while the spectra acquisition regions can be chosen to be 0.5–500 μm. The MEPHISTO spectromicroscope has been used for studies in neurobiology, including the detection of trace concentrations of metals in neuron networks, and the analysis of the boron distribution in rat brain tumor tissues [15,16].

We are currently trying to adapt the methods of immunohistochemistry for optical microscopy to spectromicroscopy. The goal is to label tissue structures with a nonphysiological element for imaging in the MEPHISTO spectromicroscope. Specifically, we intend to use the ABC (avidin-biotin-complex) technique [17] with the incorporation of nickel as a staining agent, which is spectroscopically detectable. The results of this effort have not yet been perfected and will be the subject of a further publication. The data presented below were obtained from human glioblastoma samples from patients administered with BSH and stained with nickel in the framework of this effort. Nickel staining does not affect the spectromicroscopy of boron or other physiological elements.

II. MATERIALS AND METHODS

A. XANES spectroscopy of reference boron compounds

X-ray absorption near edge structure (XANES) spectra of all compounds were acquired at the University of Wisconsin-Madison Synchrotron Radiation Center. Certain spectra were acquired from the User's Chamber on the Mark V Grasshopper or 10 m TGM beamlines, by measuring the total photocurrent from a powdered sample mounted on carbon tape. Other spectra were acquired from a sample in MEPHISTO mounted on the 6 m TGM beamline, by measuring the intensity at the phosphor screen (proportional to the total photoelectron yield) of MEPHISTO. A comparison of the energy position of the characteristic sharp peak of tetrahedral boron oxide from spectra taken on these beamlines showed discrepancies of up to 0.6 eV between the beamlines. This was compensated for by rigidly shifting spectra from the Mark V and 10 m TGM beamlines to match those from the 6 m TGM.

All spectra were saved as text files and plotted in KALEIDAGRAPH 3.0.4 for Macintosh. Normalization of the spectra was performed by dividing the experimental data by the beamline transmission curve acquired reading the photocurrent on either a gold diode (in the case of 6 m TGM) or from a piece of bare carbon tape (Mark V, 10 m TGM), which does not contain boron. The beamline transmission curve vs photon energy often contains undesirable structures which affect the spectrum lineshape, and which must be removed.

The boron compounds cesium borocaptate (BSH), cesium dodecahydrododecaborate, decaborane, *ortho*-carborane, sodium tetrahydridoborate, and boronophenylalanine were purchased from Boron Biologicals, Inc., and studied as pure powder without further purification. All other inorganic boron, sulfur and phosphorus compounds were purchased from Alfa Aesar.

Additional reference samples of BSH were prepared by depositing 2 μg BSH in solution onto a silicon substrate and air drying. To investigate the possibility of photochemical reactions induced by x-ray illumination, or other artifacts created during ashing, we also prepared BSH droplet samples in the presence of albumin. This large molecular weight protein has all the physiological elements present in the tissue, and may therefore constitute a source of chemicals necessary for such reactions. These samples were prepared with 2 μg BSH in a matrix of up to 5 μg bovine serum albumin. One BSH sample and the BSH/albumin samples were ashed in a cold oxygen plasma or UV/ozone (as described below for tissue sections) for different periods, up to 48 h.

B. Human tissue samples

The tissue samples from three patients were obtained from the Hospital St. Jürgen Str., Bremen, Germany. They are identified using the patients' initials and the number of the section taken from the tissue block. Two of the patients (FR and JU) requiring brain surgery for the removal of malignant glioblastoma were intravenously injected with BSH 24 h before the operation (patient FR) or 70 and 22 h before (patient JU was administered twice with BSH). The control sample (patient DS) was obtained from a patient who was

not administered any boron compound. The excised tumor tissue was fixed overnight in a 10% solution of formaldehyde. It was dehydrated by immersion in baths containing increasing concentrations of ethanol (70, 96, and 99 %, three exposures for 30 min at each concentration) ensuring limited exposure of tissue to ambient air while transferring between baths. The tissue was hardened in toluene for 1 h and finally embedded in paraffin at 60 °C.

Sectioning of the bulk tissue samples in paraffin was performed with microtomy (7 μm thick sections). A few sections were taken from patient JU by ultramicrotomy after embedding the tissue in resin. These sections were between 100 nm and 2 μm thick, and were not stained.

Tumor tissue containing boron was taken from two different patients. From ICP-AES analysis, the boron concentration in the tumor from patient FR was 75 ppm. ICP-AES data for patient JU were not available.

For MEPHISTO analysis, microtomed sections were mounted on silicon wafers. Neighboring tissue sections were mounted on glass microscope slides. Both the glass and silicon surfaces had been treated with ARPES [3-(triethoxysilyl)propylamine] to improve tissue adhesion. When the samples for MEPHISTO analysis were stained, this procedure was carried out simultaneously with the staining of the neighboring sections on glass to provide reference samples for visible light microscopy (VLM) analysis. If the MEPHISTO sample remained unstained then only the neighboring sections on glass were stained to provide reference samples.

The ABC (avidin-biotin-complex) staining method used here is described in detail elsewhere [17,18]. The monoclonal antibodies used for immunohistochemical staining were either anti-Ki-67 (a protein found in the nuclei of proliferating cells, antibody from Dianova, Germany), anti–van Willebrandt factor (located in blood vessel endothelia, antibody from DAKO, Denmark) or anti-BSH (prepared at the University of Bremen).

Following the removal of paraffin with xylene, the tissue sections were rehydrated with increasing concentrations of water in ethanol. In all stained samples, endogenous peroxidase was blocked with 1% H_2O_2 in double distilled water, then the specimens were incubated with normal serum (DAKO, Denmark) in a humid chamber for 1 h at room temperature. All subsequent incubations also took place in a humid chamber at room temperature. After each application of reagents, the sections were washed with 0.005 Tris-HCl buffer Ph=7.4. The samples were then incubated overnight with the monoclonal antibody.

Following the exposure to the primary antibody and washing, all samples were exposed for 30 min to a biotin-conjugated secondary antibody. Several secondary antibodies may bind to the immunoglobulin of each primary antibody. An enzyme (either horseradish peroxidase or alkaline phosphatase) was linked to the secondary antibodies via the formation of avidin-biotin-enzyme complexes in a 30 min incubation. Amplification of the stain occurs during this process, as many enzyme units bind to the secondary antibodies. The stain development process is different for the two enzymes. Oxidative polymerization of diaminobenzidine by horseradish peroxidase and H_2O_2 in the presence of $NiCl_2$ produces a black precipitate. In this way, nickel is incorporated into the stain for subsequent MEPHISTO or VLM analysis. In double stained samples for the VLM, a blue precipitate is obtained from the alkaline phosphatase mediated BCIP/NBT redox reaction.

Tissue samples from patient FR destined for MEPHISTO analysis were ashed with a cold plasma (150 °C, Plasma-Processor 300E, Techn. Plasma GmbH, München) in the presence of oxygen for 24 h. After ashing the tissue thickness is reduced because carbon and nitrogen are removed by oxygen plasma oxidation. More specifically, the atomic oxygen radicals in the plasma react with the carbon present in the tissue to form CO or CO_2, which are then removed by the pumping system. Carbon is a majoritary component of tissue, therefore removing carbon by ashing results in an enhancement of the relative concentration of the other elements (boron in the present case). We previously demonstrated the effectiveness of ashing in this respect, and we showed that no material displacement was detected [19]. The detection limits of MEPHISTO for phosphorus ($2p$) and chromium ($2p$) are on the order of 100 ppm and it is reasonable to assume a similar limit for boron ($1s$) [20]. The measured bulk concentration of boron in the human tissue samples studied is at this level or less, so that boron from BNCT is in principle undetectable by MEPHISTO in unashed tissues, at least if the boron is homogeneously distributed. The tissue samples on silicon from patient FR were ashed with UV light from a low pressure mercury lamp, which generates and dissociates ozone and consequently removes organic carbon by oxidation [21]. The ozone ions are lower in energy than the oxygen plasma, and this further ensures that no redistribution of material occurs during ashing.

The MEPHISTO spectromicroscope [13] uses an electron optics system (SpectroMicroTech, Milwaukee, WI, USA) to form a magnified image of the secondary electrons, originating from inelastic collisions of primary and Auger electrons, emitted by a specimen under soft x-ray illumination. The x-ray beam incident at 60° to the specimen normal, which lies on the electron optical axis. The electron image intensity is amplified by a series of two microchannel plates, and converted into a visible image by a phosphor screen (Galileo, Ca, USA). This image is captured by a video camera (Dage, USA) linked to a Pentium computer for display and data acquisition. The image magnification is continuously variable up to 8000 times, and the optimum lateral resolution has been measured to be 20 nm [22]. The photoelectrons are not energy filtered, so the total photoelectron yield, per unit area per unit time, is recorded as a function of photon energy. Such spectra reflect the x-ray absorption coefficient of the specimen surface and are hence referred to as x-ray absorption spectra. The depth at the specimen portion that is probed by this technique is limited by the secondary electron escape depth, which is less than 100 Å in the B $1s$ photon energy range [23]. The energy position and lineshape of spectral features provide element identification and chemical state information. Spectra can be acquired simultaneously from several regions selected anywhere on the image of the sample surface. For this work, MEPHISTO was mounted on the 10 or 6 m TGM beamlines of the University of Wisconsin-Madison Synchrotron Radiation Center.
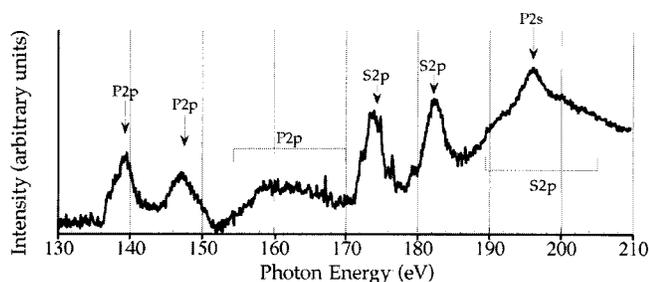
FIG. 1. X-ray absorption spectrum of UV/ozone ashed control tissue (no boron) across the sulfur and phosphorus *L* edges. The contributions from *S* and *P* indicated are typical for ashed tissue. Spectrum acquired in the MEPHISTO chamber on 6 m TGM beamline.

Optical micrographs were obtained using a Zeiss Axiotech 100 HD microscope connected to a Sony 950 DXC color video camera whose output was captured using AVID VIDEOSHOP® software for Macintosh. MEPHISTO and VLM micrographs were manipulated in ADOBE PHOTOSHOP 3.0 for Macintosh. The contrast was slightly enhanced and the scale bar added.

III. RESULTS AND DISCUSSION

A. Principles of boron detection in tissues with x-ray absorption spectroscopy

Figure 1 shows a typical total yield spectrum acquired in the photon energy range 160–210 eV from ashed brain tissue not treated with boron, containing signals from sulfur and phosphorus. The tissue was ashed for 72 h in an ozone/UV-

light environment. The spectroscopy of all principal physiological elements following ashing is reported in a separate article [21]. The B 1*s* absorption edge lies in the photon energy range 175–210 eV. There are three important contributions to the absorption spectrum in this region: (1) the strong S 2*p* shape resonance at 182 eV, (2) broader resonances between 187–200 eV also associated with the S 2*p* core level, and (3) the peak of the P 2*s* absorption edge.

1. Sulfur and phosphorus L-edge XANES

The strongly oxidizing environment during the ashing process was expected to convert all the organic sulfur and phosphorus compounds into oxides, and this was confirmed experimentally by comparing the x-ray absorption near-edge structure (XANES) spectra of reference sulfate and phosphate compounds with the spectra from ashed tissues. The results at the sulfur *L* edge are reported in Figs. 2(a) and 2(b). The near-edge region of the sulfur *L* edge has been described as a ''fingerprint'' region because the spectral structure is unique for each chemical environment [24]. Furthermore, as shown elsewhere [19], the ashing of tissues removes all detectable carbon from the probed surface layer. Figure 2 shows the XANES of a range of sulfur-oxygen-metal reference salts. The metals chosen (potassium and sodium [monovalent, Fig. 2(a)] and calcium [divalent, Fig. 2(b)]) are physiologically present in tissue. Figure 2(a) demonstrates that the main factor influencing the line shape is the chemical structure (compare sodium sulfate, sulfite, and thiosulfate) although there are also differences between the spectra from sodium and potassium sulfate. The top spectrum of calcium sulfate in Fig. 2(b) shows extra structure due to higher orders
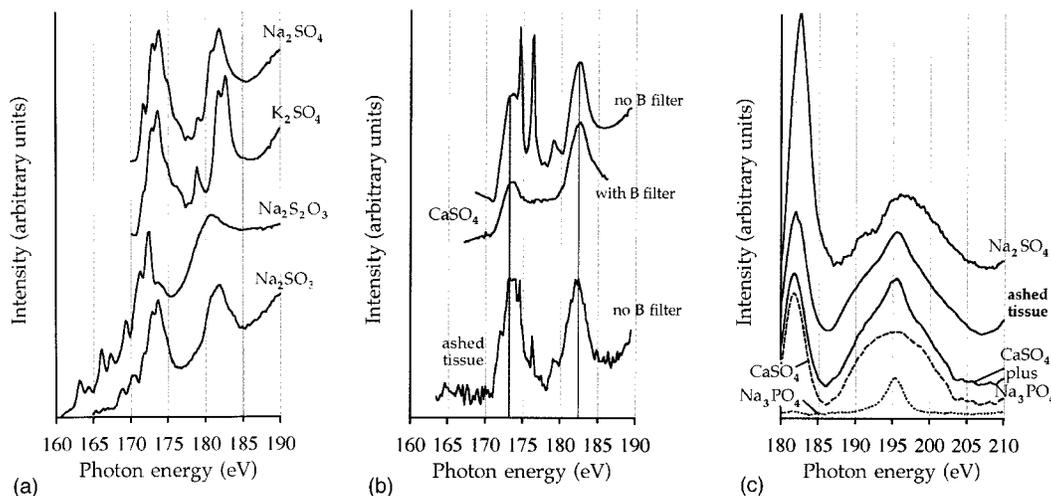

FIG. 2. Sulfur *L*-edge XANES spectra from metal-sulfur-oxygen compounds which may be formed during the ashing of tissues. The near-edge fine structure is unique for each compound and can be compared with the XANES from ashed tissue (b) to determine the products of the oxidation of organic sulfur. (a) The XANES of monovalent metal sulfates (sodium sulfate Na_2SO_4 and potassium sulfate K_2SO_4) and the lesser oxides sodium thoisulfate $Na_2S_2O_3$ and sodium sulfite Na_2SO_3. (b) Sulfur *L* edge XANES of the divalent metal sulfate calcium sulfate $CaSO_4$, acquired with and without a boron filter to remove higher order (higher energy) photons from the monochromator output. The filter removes three spurious spectral components (the sharp doublet around 175 eV is the second order calcium 2*p* signal, the peak at 179 eV is third order O 1*s*). The bottom spectrum is from UV/ozone ashed control tissue (acquired with no filter), and is closest to the top calcium sulfate line shape. Extra structure may be explained by the presence of other sulfates (a) but not the lower sulfur oxides. (c) Sulfur XANES contribute structure in the boron 1*s* energy region (175–210 eV) which is smoother for calcium sulfate than for sodium sulfate (top solid line). The lowest solid curve shows a combination of the calcium sulfate (dashed line) and a sodium phosphate peak (P 2*s*, dotted line) which very well reproduces the spectrum from ashed tissue not containing boron (central solid line). Reference spectra acquired in SRC User's Chamber on 10 m TGM beamline.

of synchrotron light, specifically second order Ca $2p$ peaks (normally at 350 eV) and another signal at 179 eV attributed to third order O $1s$ (normally at 537 eV). By using a thin boron film as a low pass filter (188 eV cutoff) in the x-ray beam, these effects were removed in the lower spectrum. Both of these spectra are presented since the boron filter could not be used when studying real tissue samples. Hence the final spectrum, taken from ashed human brain tissue, also contains these higher order signals.

Comparing the spectra in Figs. 2(a) and (b) we conclude that ashed tissue contains mostly calcium sulfate (the second order $2p$ peaks show that calcium is certainly present). The extra structure on each of the two main peaks indicates that other (potassium or sodium) sulfates are present at lower concentrations. The relative concentrations of these metals do vary throughout normal tissue, and some variation in exact line shape is observed in real samples. Although there is some noise in the tissue spectrum before the first peak, we never observed any structure below 170 eV that matched the lineshapes of the lower sulfur oxides.

The structure of the sulfur L-edge continuum resonances within the B $1s$ energy region varies with the local atomic environment of the sulfur atom (i.e., the oxygen coordination of the sulfur atom and the salt stoichiometry). Figure 2(c) compares the ashed tissue line shape with two reference sulfur spectra and one spectrum from a phosphate species. Physiological phosphorus is also oxidized during ashing and the resulting phosphates contribute structure through P $2s$ absorption at 196 eV. Figure 2(c) shows that a linear sum of the calcium sulfate and sodium phosphate spectra (shown individually as the dashed lines) agrees very closely with the spectrum from ashed tissue. By contrast, the spectrum from sodium sulfate (sodium is monovalent) clearly has extra structure around 190 eV as compared to that from calcium sulfate (calcium is divalent). Very little variation was observed in the position and shape of the P $2s$ peak in other phosphates. However, the intensity ratio of sulfur and phosphorus signals can fluctuate significantly across the surface of a tissue section [compare Fig. 2(c) with the same energy region of Fig. 1]. *In vivo*, regions of protein synthesis are richer in sulfur than, for example, the nucleus, which contains nucleic acids, in turn rich in phosphates. In general, however, a linear combination of a sulfate $2p$ signal and a phosphate $2s$ signal is a good model for the absorption spectrum of ashed control tissue in the B $1s$ region (175–210 eV).

These spectra indicate that the interference between sulfur and boron are minimized if the tissue is fully ashed (i.e., physiological sulfur is fully oxidized to sulfate) and if the predominant species is calcium sulfate or the sulfate salt of another divalent metal. The sulfur L-edge spectra are then smooth in the B $1s$ energy region.

2. Boron K-edge XANES

We acquired reference spectra from relevant boron compounds to understand the boron absorption spectra acquired from tissues.

Mercaptoundecahydrododecaborate (the sulfhydryl boron hydride, $B_{12}H_{11}SH$ or BSH). BSH has a *closo* icosahedral (12 atom) boron framework covered by *exo* hydrogen atoms, with the exception of the -S-H group substituted for hydro-
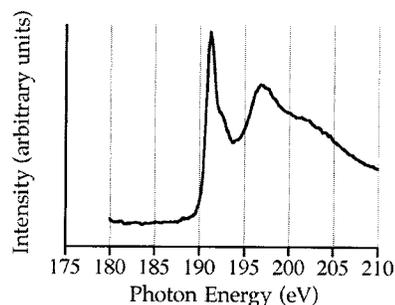

FIG. 3. Boron K edge XANES of $B_{12}H_{11}SH$. Spectra acquired in the MEPHISTO chamber on 6 m TGM beamline.

gen. The icosohedral moiety has an overall charge of 2^-, and hence is soluble in water and forms ionic salts (e.g., Cs_2BSH or Na_2BSH). The spectrum of BSH is displayed in Fig. 3.

Boron oxides. As the ashing of organic sulfur and phosphorus compounds is expected to form sulfates and phosphates, so the boron in BSH may also be oxidized. Boron naturally forms oxides with a range of stoichiometric formulas, but the most common structural unit contains boron coordinated by oxygen atoms in a planar trigonal environment. This is the case for both the crystalline oxide B_2O_3, and boric acid $B(OH)_3$. The identical K-edge XANES spectra of these compounds are displayed together in Fig. 4.

Ashing BSH. To follow the chemical changes produced in BSH present in tissue during ashing, BSH in solution (2 μg) was deposited onto silicon substrates and air dried, either pure or in the presence of 1 μg bovine serum albumin (BSA), and these were ashed for up to 48 h. A cold oxygen plasma oven was used to ash these specimens. The energetic oxygen ions in plasma are expected to oxidize samples more rapidly then the UV/ozone environment (in which the oxygen radicals have thermal kinetic energies) but the chemical endpoint will be the same. When BSH was ashed alone an oxide species was rapidly formed, as shown by the characteristic sharp peak at 194 eV, having a maximum intensity after about 1 h [Fig. 5(a)]. The intensity of the BSH 191.4 eV exciton was also reduced. However, the oxide peak subsequently diminished, as seen in the 48 h spectrum.

When BSH was ashed in a protein matrix, the strength of the boron signal increased with ashing time, as organic carbon was removed [Fig. 5(b)]. In this case the oxide peak
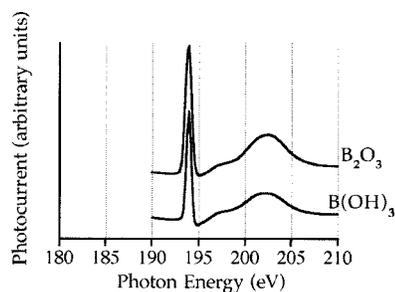

FIG. 4. Boron K edge XANES of boron oxide B_2O_3 and boric acid $B(OH)_3$. The structures of these compounds are similar (boron is trigonally coordinate with oxygen in both cases) giving indistinguishable spectra. Spectra acquired in SRC User's Chamber on Mk V Grasshopper beamline.
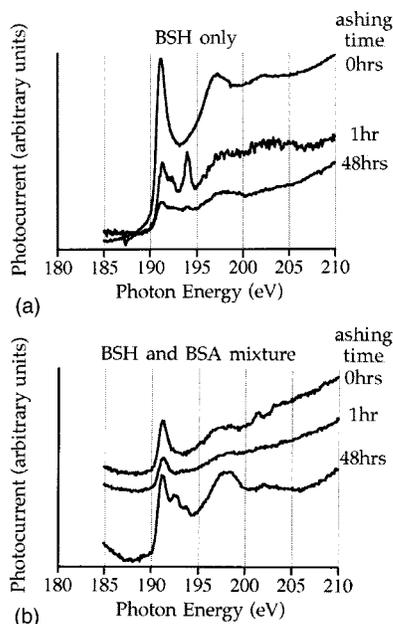
(a)

(b)

FIG. 5. Boron *K* edge XANES of reference 2 μg BSH samples ashed for up to 48 h in a cold oxygen plasma. (a) Ashing pure BSH crystals. (b) Ashing BSH in a protein matrix [1 μg bovine serum albumin (BSA)]. Spectra acquired in the MEPHISTO chamber on 6 m TGM beamline.

never develops strongly, and the additional peak at 192.5 eV appears after 12 h, remaining until 48 h.

These data suggest that the BSH cage is attacked during ashing to form boron oxide. However, boron oxide was observed to be volatile in vacuum (and in air above 100 °C). The reduction in the strength of the oxide peak, and the overall boron signal then indicates that boron (as the oxide) might be removed from the sample, either during ashing, or later under vacuum. A protein matrix appears to stabilize the BSH molecule, however, as the line shape and relative intensities of the boron XANES spectra in Fig. 5(b) show much less oxidation. Note that a parallel series of carbon spectra was acquired (not shown) and after 48 h ashing no carbon was detected.

B. Spectroscopy of boron in human glioblastoma tissue

1. BSH in tissue

The data presented in Sec. I demonstrate the potential difficulties in the detection of trace quantities of boron (as BSH) in tissue by x-ray absorption spectroscopy in MEPHISTO. (1) Ashing of the tissue is required to raise the relative expected boron concentrations for its detection, but this may cause the loss of boron from the sample as the oxide. (2) Sulfur and phosphorus are both interferences in the x-ray energy region of interest. The main concern is with S 2p continuum resonances above 187 eV. We have shown that the products of the ashing process are sulfates, and that calcium sulfate gives a smooth signal above 187 eV, which could not be misinterpreted as a B 1s signal. Other sulfates may be present in tissues, however, which do have spectral structure in the B 1s energy region.

Given these constraints, we studied real tissue samples from brain tumor patients administered with BSH. With ref-
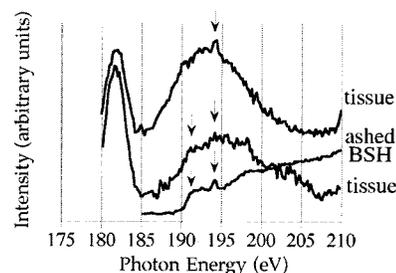

FIG. 6. XANES spectra from ashed tissue containing BSH showed two structures (shown by arrows) that match those in the ashed BSH reference spectra and which are not due to phosphorus or sulfur. The two tissue spectra reported indicate that BSH in tissue may not be oxidized to the same extent between ashed samples as while the top curve exhibits a strong boron oxide peak, the lower curve additionally shows structure at 191 eV. Ashed tissue spectra acquired in the MEPHISTO chamber on 6 m TGM beamline.

erence to the spectra of Figs. 5(a) and 5(b), BSH in ashed tissue should be detected via either the BSH or oxide exciton peaks (at 191.1 and 194 eV), or as a step centered at 190.5 eV [see the 48 h ashing curve in Fig. 5(a)]. Both peaks are narrower than any sulfur component in this region, and are clearly separated from the phosphorus 2s signal. If ashing removes both of these peaks the spectra of boron in tissue, however, the remaining absorption step lies very close to the step observed in the sodium sulfate spectrum.

MEPHISTO analysis of tissue containing BSH gave spectra containing the signature of ashed BSH as identified by the two features indicated by arrows in Fig. 6. The top tissue spectrum clearly possesses the boron oxide resonance at 194 eV, while the lower tissue spectrum has a shoulder at 191 eV and a weak 194 eV resonance in close agreement with the ashed BSH spectrum included for reference. Neither of these structures was ever seen in control tissue not containing BSH [Fig. 2(c)]. We observe the expected boron features, but also conclude that the extent of oxidation of the BSH molecule due to ashing may vary between samples.

2. An alternative boron chemical state

In approximately 40% of the 130 microscopic areas analyzed across the three tissue samples we found evidence of a boron signal at 188.3 eV. This was reproducible in two different patients and absent from the control case. Figure 7 shows two examples of these results, taken from glioblas-
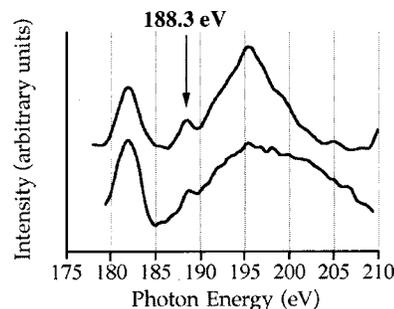

FIG. 7. XANES spectrum of UV/ozone ashed tissue from two human patients which clearly show a peak at 188.3 eV in addition to the contributions from sulfate and phosphate. Spectrum acquired in the MEPHISTO chamber on 6 m TGM beamline.

TABLE I. Frequency table reporting the detection of the 188.3 eV peak from sections from three patients. Each count represents one unique tissue area from which an x-ray absorption spectrum in the boron $1s$ energy range was acquired. The notation *vWf* in the second column indicates that the tissue had been stained against van Willebrandt factor.

Patient and Sample(s)	Sectioning	Staining	No. of regions with 188.3 eV peak	No. of regions with no 188.3 eV peak
DS 1 (control)	microtomed	unstained	0	7
JU U1–U4	ultramicrotomed	unstained	3	10
JU 265	microtomed	*vWf*	8	10
JU 268	microtomed	*vWf*	14	17
FR 41	microtomed	unstained	12	49

toma tissue from patient JU, section 265 (top curve) and from patient FR, section 41 (bottom curve). In this spectrum, in addition to the sulfur and phosphorus contributions seen previously (the P $2s$ peak is very weak in the lower curve), there is a sharp peak at 188.3 eV. This peak is too sharp to be a sulfur $2p$ high-energy resonance, and has never been seen in the absorption spectra of sulfur compounds studied by our or other groups [25]. It is also too low in energy to be associated with the phosphorus $2s$ peak, and could not be attributed to higher diffraction order structures from the beamline or other artifacts associated with the x-ray beam. Only boron could give a peak at this energy, although it is in a reduced oxidation state compared to boron in BSH. It is commonly observed in both x-ray absorption and photoemission spectroscopy that core level energies can increase as oxidation number increases. The oxidation-induced withdrawal of valence electrons that penetrate into the atom reduces nuclear charge screening and therefore increases the binding energies of core levels. In the present case, boron appears to be reduced, as the 188.3 eV B $1s$ binding energy is lower than in boron oxide or BSH.

The x-ray absorption spectra of many boron compounds were acquired to investigate the origin of this signal, but so far we did not observe any boron absorption features below 189 eV. Nevertheless, a boron $1s$ peak is the only reasonable description of this signal. A review of the literature pertaining to boron x-ray absorption spectroscopy revealed one possible interpretation. McLean *et al.* formed a subsurface layer of boron in an annealed silicon wafer heavily doped with boron [26]. Boron in this sample had a peak at 188.6 eV in the absorption spectrum.

It is unlikely that we have reproduced the physical situation reported by McLean *et al.*, which would have required boron atoms to diffuse past the top silicon layer. In addition, we do not expect *a priori* that the underlying silicon substrate on which the tissue samples are placed should be spectroscopically visible in MEPHISTO, as the probing depth is less than 100 Å. However, McLean's result demonstrates that boron in a reduced chemical state can have x-ray absorption peaks at lower energies than BSH and the other compounds studied. Boron may be bonded to one or more other elements physiologically present in the tissue that generate a boron chemical state with the observed peak at 188.3 eV. We have not yet identified this compound, but the results of McLean *et al.* prove that it is plausible.

Another possible interpretation for the appearance of the peak at 188.3 eV is that boron in BSH is reduced under x-ray illumination during the MEPHISTO experiments. To exclude this possibility, we carefully analyzed BSH in the presence or absence of albumin, before and after ashing. The results are presented in Figs. 5(a) and 5(b) and discussed in **A**. In none of these cases did such a structure appear under illumination.

These experiments also demonstrate that the formation of the 188.3 eV peak cannot have occurred during the ashing procedure, as a result of ionization and subsequent reaction of boron with other physiological elements, provided in this test by albumin. The presence of the 188.3 eV peak cannot be a consequence of the presence of nickel in the tissue, as it has been observed in samples from two patients, both containing and not containing nickel. Ni $2p$ peaks are at 853 and 870 eV, and Ni $3p$ peaks are at 66 and 68 eV, very far from 188.3 eV and therefore without interference in this energy region. Table I summarizes the frequency with which this signal was observed. The boron signal at 188.3 eV was not seen everywhere in the FR and JU cases. This suggests that the boron distribution in tumor, following administration of BSH, is inhomogeneous.

The existence of a boron absorption peak at 188.3 eV, and the absence of BSH spectral features suggests that a change in the chemical state of boron has occurred *in vivo*. Such a peak could be interpreted as an artifact introduced by the ashing procedure, but we have shown that oxidation of BSH leads to higher energy features. This is true also when BSH is ashed in the presence of albumin. Another possible cause could be photoreduction in the synchrotron beam, although photochemistry was never observed in reference BSH depositions on silicon, even in the presence of albumin. The only hypothesis that is not contradicted by the experimental results is the chemical modification of the BSH anion *in vivo*.

3. Microlocalization of boron signals in tissue

The tissue section JU 265 was accompanied by a neighboring tissue section on a glass slide that was double stained against van Willebrandt factor (to locate blood vessel endothelia) and against molecular BSH. The results of the anti-BSH staining showed both a diffuse positive staining throughout some tissue areas (a small fraction of the total tissue area, with typical dimensions of $100 \times 400 \, \mu$m) and small localized denser spots having a diameter of 5–10 microns, in the same areas. Positive staining against BSH oc-
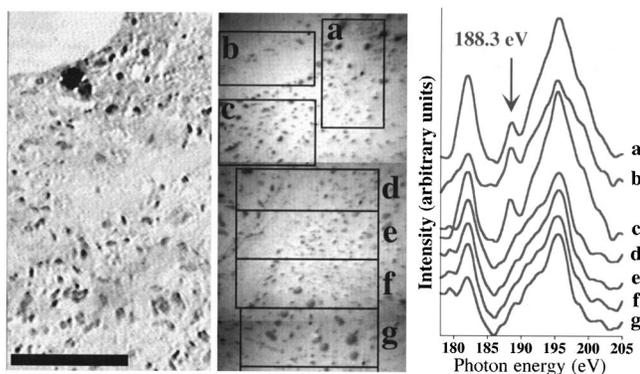
FIG. 8. Left. (Patient JU, section 269) optical micrograph of human glioblastoma section mounted on a glass slide and double stained against van Willebrandt factor and BSH. A diffuse positive stain for BSH was developed at the lower edge of the gap in the tissue. The scale bar (black, at bottom)$=100\ \mu$m. Center. (Patient JU, section 265) composite MEPHISTO photoelectron micrograph of the equivalent tissue area to that shown on the left. The area studied corresponds to the most darkly stained region of tissue seen in the left image, at the edge of the gap, and moving down the tissue away from the edge. The photon energy was 139 eV. Right. X-ray absorption spectra were acquired in each one of the boxes indicated in the center micrograph. Note that the regions (a)–(c) which show most strongly the B $1s$ peak at 188.3 eV correspond to the regions that showed positive staining against BSH.

curred only in well vascularized areas (as proven by the staining against van Willebrandt factor) although not all stained blood vessels could be associated with BSH penetration into the tumor.

The 188.3 eV boron species was observed only in the tissue areas that were well vascularized and which gave positive anti-BSH staining. Absorption spectra from these areas showed too much phosphorus interference to clearly characterize the BSH distribution with MEPHISTO. The 188.3 eV peak is clearly separated from the P $2p$ peak, however, and could be traced through the tissue as demonstrated by Fig. 8.

The image on the left of Fig. 8 is an optical micrograph (patient JU, section 269) showing the positive stain (blue in the original image, a darker gray in this version) against BSH at the border of a gap in the tissue. This gap was seen in several consecutive tissue sections, and so is not an artifact of the sectioning process. The equivalent tissue region was studied in MEPHISTO on section 265 (that is, a section that was taken by microtomy from the same tissue block four sections (28 μm) before the section for VLM imaging). A composite image constructed from photoelectron micrographs (acquired with a photon energy of 139 eV, the maximum of the P $2p$ absorption) is shown at the center of Fig. 8. The boxes in this image represent the acquisition areas from which the correspondingly labeled absorption spectra reported on the right were acquired. There is a gradual modulation in the 188.3 eV peak intensity over the $100\times400\ \mu\text{m}^2$ region of this image.

In previous studies, positive staining against BSH was observed in localized spots similar to those found in our cases, JU and FR [17]. Double stained samples against BSH and Ki-67, a protein found in the nuclei of proliferating cells, showed examples in which both stains overlapped at some regions, indicating that BSH is actually accumulated in some

nuclei. This result has also been published independently by secondary ion mass spectrometry (SIMS) [12]. A motivation of the analysis of these tissue samples with spectromicroscopy is to investigate whether the immunohistochemical stainings for the optical microscope do show that BSH is accumulated inside nuclei. At present, the very weak boron signal in MEPHISTO (at 188.3, 191, or 194 eV) does not allow a direct comparison with the results of immunohistochemical staining.

V. CONCLUSIONS

The work presented here represents the first systematic application of chemical analysis with XANES spectroscopy to human tissue samples. The specific aim of this work is to discover the microdistribution and chemical state of boron in human tissue samples treated with BSH for BNCT. We have shown that the products of tissue ashing can be identified by comparing near edge structure in the x-ray absorption spectra from ashed tissue with those from reference compounds. Physiological elements which are not removed by ashing (sulfur and phosphorus) can act as interferences for boron, but the spectra we have acquired on control and reference samples allow us to identify a small signal in a real tissue sample which can be unambiguously interpreted as ashed BSH.

Samples of human glioblastoma tissue from two patients administered with BSH and one patient not administered with BSH were analyzed in the MEPHISTO spectromicroscope. A spectroscopic analysis of microscopic tissue regions discovered a weak BSH signal. Boron was found in a reduced chemical state (with respect to boron in BSH) as shown by the x-ray absorption peak at 188.3 eV. This peak was found across 40% of the tissue regions analyzed and never from the control patient. The tissue samples analyzed in MEPHISTO were prepared in parallel with a nearby section mounted on a glass slide and stained anti-BSH for VLM analysis. The reduced boron species was found in tissue in the same general areas which stained positive for BSH in VLM. The x-ray absorption feature at 188.3 eV could not be produced by ashing, nor with x-ray induced photochemistry. A proportion of the BSH injected into the patient must, therefore, have been bound or metabolized *in vivo*. The remaining proportion was not metabolized, and was immunohistochemically stained, but was only weakly detectable in MEPHISTO after ashing, and suffered interference from the phosphorus signal.

In conclusion, the present work presents evidence of *in vivo* metabolism of BSH to a different chemical state. The boron compound formed has not been yet identified, but it is plausible that BSH cage is opened *in vivo* or binds another element or molecule physiologically present in the tissue.

---

[1] F. B. Furnari, H.-J. Su Huang, and W. K. Cavanee, Cancer Surv. **25**, 233 (1995).

[2] G. L. Locher, Am. J. Roentgenol. **36**, 1 (1936).

[3] R. F. Barth, A. H. Soloway, R. G. Fairchild, and R. M. Brugger, Cancer **70**, 995 (1992).

[4] A. H. Soloway, in *Advances in Neutron Capture Therapy*, edited by A. H. Soloway, R. F. Barth, and D. E. Carpenter (Plenum, New York, 1993).

[5] A. H. Soloway, H. Hatanaka, and M. A. Davis, J. Med. Chem. **10**, 714 (1967).

[6] H. Hatanaka and Y. Nakagawa, Int. J. Radiat. Oncol. Biol. Phys. **28**, 1061 (1994).

[7] D. Gabel, in *Progress in Neutron Capture Therapy for Cancer*, edited by B. J. Allen (Plenum, New York, 1992).

[8] D. Haritz, D. Gabel and R. Huiskamp, Int. J. Radiat. Oncol. Biol. Phys. **28**, 1175 (1994).

[9] A. H. Soloway, W. Tjerks, B. A. Barnum, F.-G. Rong, R. F. Barth, I. M. Codogni, and J. G. Wilson, Chem. Rev. **98**, 1515 (1998).

[10] C. P. Ceberg, A. Persson, A. Brun, R. Huiskamp, A.-S. Fyhr, B. R. R. Persson, and L. G. Salford, J. Neurosurg. **83**, 86 (1995).

[11] D. Haritz *et al.*, in *Boron-Neutron Capture Therapy: Towards Clinical Trials of Glioma Treatment*, edited by D. Gabel and R. Moss (Plenum, New York, 1992).

[12] K. Haselsberger, H. Radner, W. Gössler, C. Schlagenhaufen, and G. Pendl, J. Neurosurg. **81**, 714 (1994).

[13] G. De Stasio, M. Capozi, G. F. Lorusso, P.-A. Baudat, T. C. Droubay, P. Perfetti, G. Margaritondo, and B. P. Tonner, Rev. Sci. Instrum. **69**, 2062 (1998).

[14] W. Gudat, and C. Kunz, Phys. Rev. Lett. **29**, 169 (1972).

[15] G. De Stasio and G. Margaritondo, in *Spectromicroscopy with VUV Photons and X-Rays*, special issue of J. Electr. Spectr. Relat. Phenom., edited by H. Ade (Elsevier, Amsterdam, 1997).

[16] B. Gilbert, J. Redondo, P.-A. Baudat, G. F. Lorusso, R. Andres, E. G. Van Meir, J.-F. Brunet, M.-F. Hamoud, T. Suda, Delio Mercanti, M. T. Ciotti, T. C. Droubay, B. P. Tonner, P. Perfetti, G. Margaritondo, and Gelsomina De Stasio, J. Phys. D **31**, 2642 (1998).

[17] B. Otersen, D. Haritz, F. Grochulla, M. Bergmann, W. Sierralta, and D. Gabel, J. Neuro-Oncol. **33**, 131 (1997).

[18] *Immunocytochemistry: A Practical Approach*, edited by J. E. Beesley (IRL, Oxford 1993).

[19] G. De Stasio, M. Capozi, T. C. Droubay, D. Mercanti, M. T. Ciotti, G. F. Lorusso, R. Andres, T. Suda, P. Perfetti, B. P. Tonner, and G. Margaritondo, Anal. Biochem. **252**, 106 (1997).

[20] F. J. Esposto, P. Aebi, T. Tyliszczak, A. P. Hitchcock, M. Kasrai, J. D. Bozek, T. E. Jackman, and S. R. Rolfe, J. Vac. Sci. Technol. A **9**, 1663 (1991).

[21] G. De Stasio, B. Gilbert, L. Perfetti, R. Hansen, D. Mercanti, M. T. Ciotti, R. Andres, P. Perfetti, and G. Margaritondo, Anal. Biochem. **266**, 174 (1999).

[22] G. De Stasio, L. Perfetti, B. Gilbert, O. Fauchoux, M. Capozi, P. Perfetti, G. Margaritondo, and B. P. Tonner, Rev. Sci. Instrum. **70**, 1740 (1999).

[23] M. Kasrai, W. N. Lennard, R. W. Brunner, G. M. Bancroft, J. A. Bardwell, and K. H. Tan, Appl. Surf. Sci. **99**, 303 (1996).

[24] M. Kasrai, J. R. Brown, G. M. Bancroft, Z. Yin, K. H. Tan, and X. Feng, Int. J. Coal Geol. **32**, 107 (1996).

[25] M. Kasrai, Z. Yin, and G. M. Bancroft, J. Vac. Sci. Technol. A **11**, 2694 (1993).

[26] A. B. McLean, L. J. Terminello, and F. J. Himpsel, Phys. Rev. B **41**, 7694 (1990).